Supporting Information

Plasmonic imaging of electrochemical oxidation of single nanoparticles

Yimin Fang[1], Wei Wang*[1], Xiang Wo[1], Yashuang Luo[1], Shaowei Yin[1], Yixian Wang[2], Xiaonan Shan[2], and Nongjian Tao*[1,2]

1. State Key Laboratory of Analytical Chemistry for Life Science, School of Chemistry and Chemical Engineering, Nanjing University, Nanjing 210093, China.

2. Center for Bioelectronics and Biosensors, Biodesign Institute, Arizona State University, Tempe, AZ 85287, USA.

* Corresponding Authors:

W.W., e-mail: wei.wang@nju.edu.cn;

N.J.T., e-mail: njtao@asu.edu

1. Experimental section:

Materials. The Ag nanoparticles used for performing electrochemical experiments were synthesized by the classical citrate reduction method. Briefly, 50 mL of 1 mM $AgNO_3$ solution was heated to the boiling point in a flask while stirring. Then 1mL 1% (wt) trisodium citrate was added to the flask and heated for one hour to obtain citrate stabilized Ag nanoparticles. The average size of the as-prepared Ag nanoparticles was about 76 nm (see Figure S2). The cysteine protected Ag nanoparticles was prepared by incubating as-prepared Ag nanoparticles in the presence of 20 μM cysteine for 2 hours in prior to experiment at room temperature. The CV curves of both unprotected Ag nanoparticles and cysteine protected Ag nanoparticles immobilized on a gold electrode are provided in Figure S4. The deionized water (18.2 MΩ) produced by Smart2Pure 3 UF (Thermo Fisher) was used for the whole experiment.

The Ag nanoparticles used for the calibration curve of size and SPR intensity were purchased from Sigma with a labeled diameter of 40, 60, 100 and 157 nm, respectively. The Ag nanoparticles are kept in aqueous buffer, contain sodium citrate as stabilizer. Compared to the homemade Ag nanoparticles, the purchased ones are also stabilized by citrate. The actual sizes are calibrated by dynamic light scattering (DLS) measurements and actomic force microscope (AFM), respectively.

Apparatus. The P-ECM setup was built on an inverted optical microscopy (TIRFM, Olympus IX-81). The light source used here was a *p*-polarized light from a 680 nm superluminescent light-emitting diode (SLED). The output power of the light source is 1 mW. 47nm-thick gold film coated on a glass coverslip was used as the working electrode and SPR sensor chip. A potentiostat (Pine Instruments, Model AFCBP1) was used to control the electrode potential with Ag/AgCl(3M KCl) and Pt coils as reference electrode and counter electrode, respectively. DLS (Malvern Nanosizer), TEM (JEM-2100, JEOL) and AFM (Agilent scanning probe microscope 5500) were used to characterize both the homemade and commercial Ag nanoparticles (see Figure. S2 and S3).

2. Oxidation kinetics:

According to the Tafel equation, the oxidation current of the nanoparticle is given by,

$$i(t) = 4\pi r^2(t) \cdot nF \cdot k_0 \cdot e^{\alpha \frac{nF}{RT}(E-E_0)}, \quad \text{(S1)}$$

where $i(t)$ and $r(t)$ are the transient current and radius of the nanoparticle, n is the number of electron transfer per atom, F is the Faradic constant, k_0 is the electron transfer rate constant, α is the charge transfer coefficient, R is the gas constant, T is temperature, E is the applied potential and E_0 is the formal potential, respectively. The amount of charge transfer is equal to the number of dissolved (oxidized) Ag atoms from the particles, so we have

$$i(t) = \frac{dQ}{dt} = \frac{d(eN_A\rho 4\pi r^3 / 3m_{Ag})}{dt}, \quad \text{(S2)}$$

where ρ, m_{Ag}, and N_A are density of silver, mass of silver atom and Avogadro's constant, respectively, and t_D is time that takes to completely oxidize and dissolve an Ag nanoparticle. If we assume the dissolution process is isotropic, then

$$i(t) = \frac{1}{m_{Ag}} eN_A \rho 4\pi r(t)^2 \frac{dr}{dt}. \qquad \text{(S3)}$$

Combining Equations (S1) and (S3), we have

$$r(t) = r_0 - \frac{m_{\text{Ag}} N_A}{\rho} k_0 e^{\alpha \frac{nF}{RT}(E-E_0)} t, \qquad \text{(S4)}$$

where r_0 is the initial radius of the nanoparticle, k_0 is the electron transfer rate constant.

Combining Equations (S1) and (S2), we have

$$\frac{dr(\mathrm{t})}{dt} = -\frac{m_{\text{Ag}} N_A}{\rho} k_0 \cdot e^{\alpha \frac{nF}{RT}(E_i + vt - E_0)}, \quad \text{(S5)}$$

where E_i is the initial potential, and v is sweeping rate, Solving the above equation, we obtain,

$$r(t) = r_0 + \frac{c}{bv} \cdot e^{b(E_i - E_0)} - \frac{c}{bv} \cdot e^{b(E_i + vt - E_0)}, \qquad \text{(S6)}$$

where $b = \alpha \frac{nF}{RT}$ and $c = \frac{m_{\text{Ag}} N_A}{\rho} k_0$. If $E_i << E_0$, we have

$$r(t) = r_0 - \frac{c}{bv} \cdot e^{b(E_i + vt - E_0)}. \quad \text{(S7)}$$

The current reaches a peak at $\frac{di(t)}{dt} = 0$. Applying this condition to equation (S1) we have,

$$E_p = E_0 + \frac{1}{b}\ln\left(\frac{r_0 b v}{3c}\right) = E_0 + \frac{2.303RT}{\alpha nF}\log_{10}\left(\frac{r_0 v \alpha nF\rho}{3RTm_{Ag}N_A k_0}\right). \qquad \text{(S8)}$$

3. Electrochemical oxidation of Ag nanoparticles with and without SCN$^-$ at low and high potentials

To examine the effect of SCN$^-$ in the electrochemical oxidation of Ag nanoparticles (Ag NPs), we carried out the measurement in 0.3 M NaClO$_4$ and the image intensity vs. time is plotted as black line in Fig. S1a. It shows that the Ag nanoparticles did not disappear (dissolve) in the absence of KSCN. For comparison, the image intensity of a Ag NP in 0.3 M KSCN is also shown (red line). Fig. S1b plots the image intensity profile of a Ag NP in 0.3 M KSCN at two different potentials, -0.2 V (red line) and -0.05 V (black line), which shows that the Ag NP oxidizes and dissolves in 0.3 M KSCN only if the potential sufficiently high.

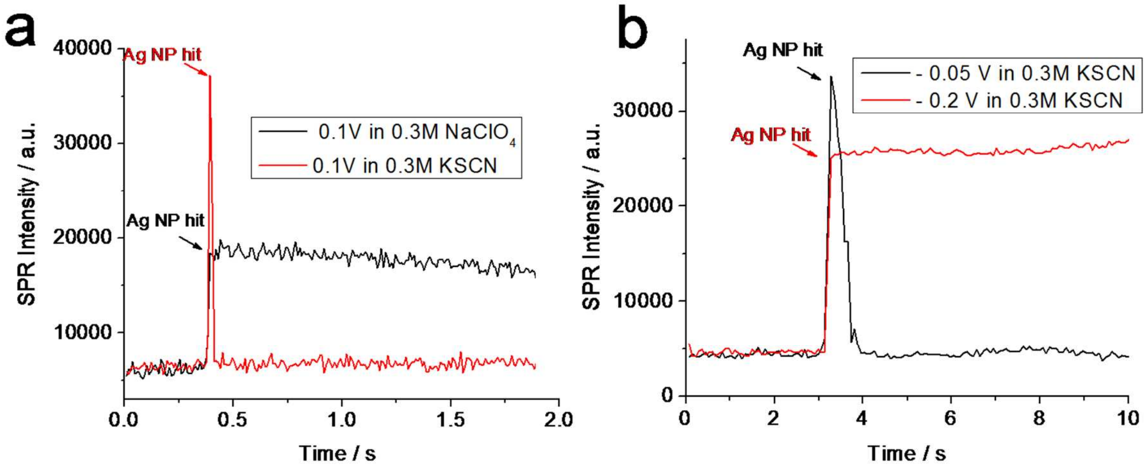

Figure S1. (a) Transient SPR image intensity of a Ag nanoparticle (Ag NP) during its collision with gold electrode in 0.3 M NaClO$_4$ (black line) and 0.3 M KSCN (red line) at 0.1 V, (b) Transient SPR image intensity of a Ag nanoparticle during its collision with gold electrode in 0.3 M KSCN at -0.2 V (red line) and at -0.05 V (black line).

4. Characterization of Ag nanoparticles

Ag nanoparticles were analyzed by both transmission electron microscopy (TEM) and dynamic light scattering (DLS) (Fig. S2). TEM analysis gives an average diameter of 76 ± 30 nm. The hydrodynamic diameter measured by DLS is 85 ± 20 nm. Additionally, AFM was also used to determine the size of a single nanoparticle, and compare with the SPR image intensity of the same nanoparticle (Fig. S3).

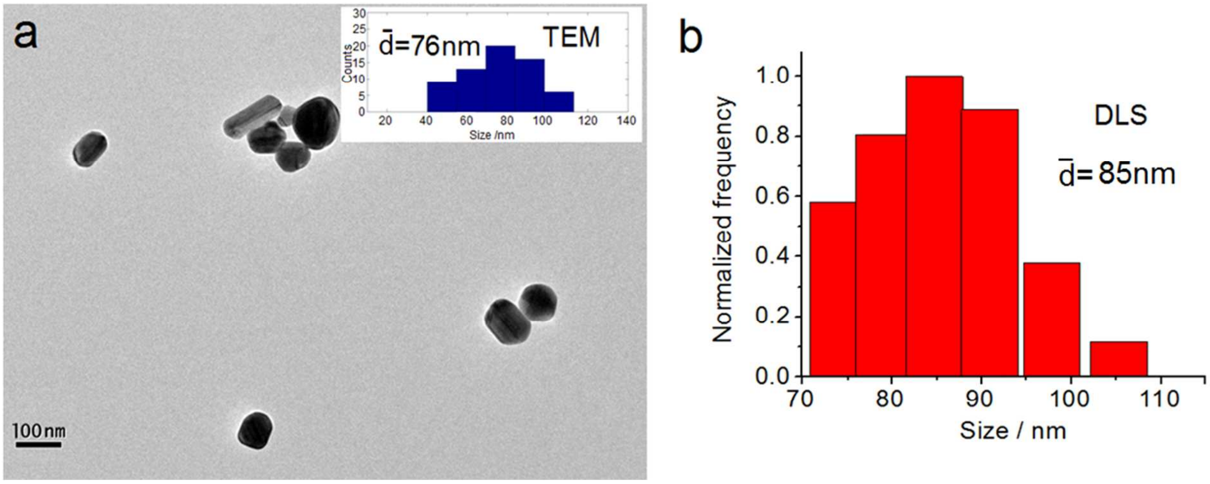

Figure S2. (a) TEM image and size distribution (inset) of Ag nanoparticles. (b) DLS of the size distribution of Ag nanoparticles.

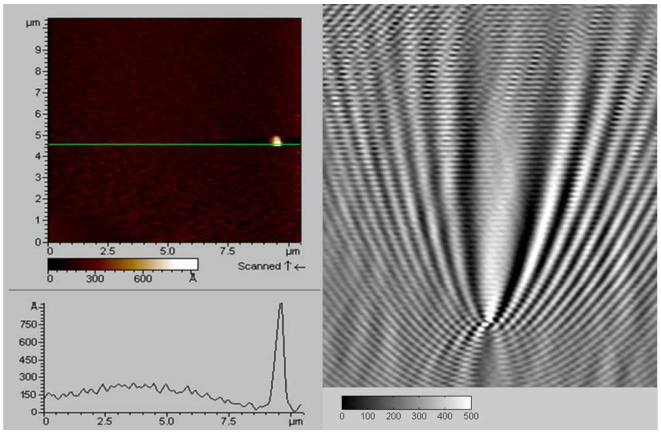

Figure S3. AFM image (left) and the corresponding SPR image (right) of a single Ag nanoparticle.

5. Effect of cysteine passivation studied by conventional electrochemical recording

We obtained traditional cyclic voltammograms of unmodified Ag nanoparticles (black line) and cysteine passivated Ag nanoparticles on gold electrodes (Figure S4). The peak oxidation potential of the cysteine-passivated Ag nanoparticles is higher than that of the unpassivated Ag nanoparticles, indicating that the surface chemistry affects the electrochemical oxidation of the nanoparticles.

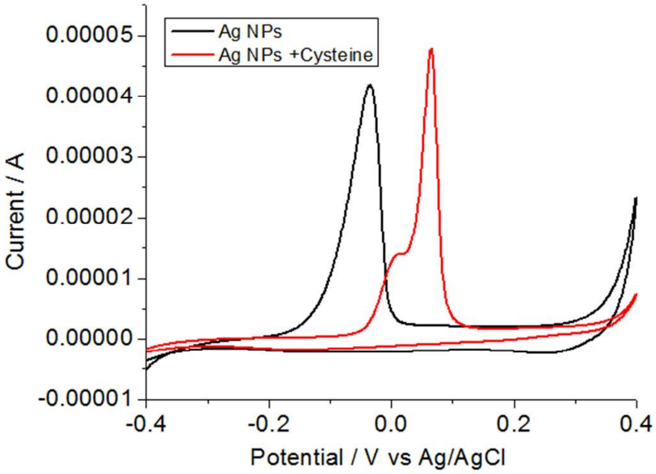

Figure S4. Traditional cyclic voltammograms of Ag nanoparticles (black line) and cysteine protected Ag nanoparticles (red line) on gold electrodes in 0.3 M KSCN. Potential sweep rate: 20mV/s.

6. Data analysis

Accurate measurement of the SPR image intensity of Ag nanoparticles is critical for quantitative analysis of electrochemical current. Because the SPR image of a nanoparticle in real has a parabolic tail, the local intensity is sensitive to the selection of the region of interest within the parabolic pattern (Figure S5a). To overcome this difficulty, the real space image was transformed into the Fourier space (Figure S5b), which displays two well defined circular rings. The intensity of each ring provides more accurate determination of the SPR image intensity.

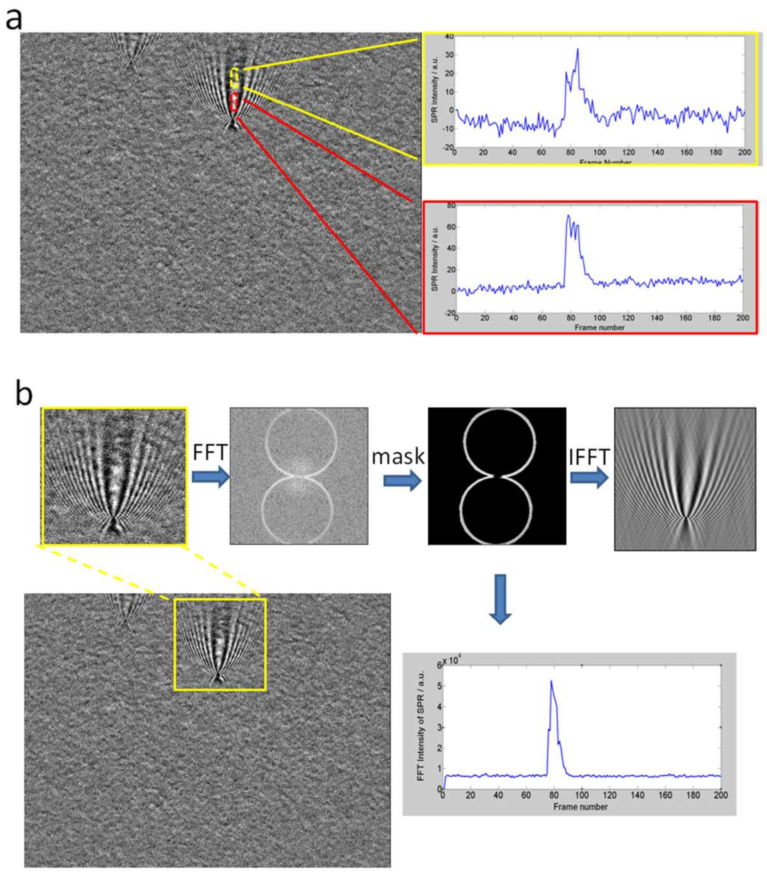

Figure S5. (a) Analysis of SPR image in real space depends on the selection of different regions of interest. (b) Analysis of SPR image in Fourier space (Fourier transform of the real space image) provides more reliable quantification of the image intensity.

7. Slope of the dissolution curve vs. oxidation potential

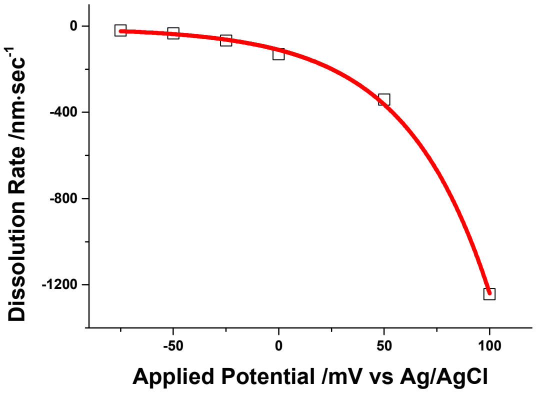

Figure S6. Slope of the dissolution curve in Figure 3C vs. the oxidation potential.

The average dissolution rate of Ag nanoparticles was found to exponentially increase with the increasing potential. This trend was in excellent agreement with Equation 2.

8. Descriptions of movies

Movie S1. Collision and oxidation of three Ag nanoparticles (potential: -50 mV, and electrolyte: 0.3 M KSCN). --------------[**File name:** ja507097y_si_002.mpg]

Movie S2. Collision and oxidation of Ag nanoparticles (potential: 0 mV, and electrolyte: 0.3 M KSCN). --------------[**File name:** ja507097y_si_003.mpg]

Movie S3. Collision and oxidation of Ag nanoparticles (potential: -200 mV, and electrolyte: 0.3 M KSCN). --------------[**File name:** ja507097y_si_004.mpg]

Movie S4. Collision and oxidation of Ag nanoparticles (potential: 100 mV, and electrolyte: 0.3 M $NaClO_4$). --------------[**File name:** ja507097y_si_005.mpg]

Movie S5. Linear sweep of potential from -300 mV and +200 mV for Ag nanoparticles (sweep rate: 20 mV/s, and electrolyte: 0.3 M KSCN). --------------[**File name:** ja507097y_si_006.mpg]

Movie S6. Linear sweep of potential from -300 mV and +200 mV for unpassivated (left) and passivated with cysteine (right) Ag nanoparticles (sweep rate: 20 mV/s, and electrolyte: 0.3 M KSCN). --------------[**File name:** ja507097y_si_007.mpg]